Peer-reviewed version available at *Appl. Sci.* **2020**, *10*, 5813; doi:10.3390/app10175813

Article

Bayesian Calibration of Hysteretic Parameters with Consideration of the Model Discrepancy for Use in Structural Health Monitoring

Rosario Ceravolo[1], Alessio Faraci[1] and Gaetano Miraglia[1,*]

[1] Politecnico di Torino, Department of Structural, Building and Geotechnical Engineering & Responsible Risk Resilience interdepartmental Centre Corso Duca degli Abruzzi, 24 -10129 Turin, Italy; rosario.ceravolo@polito.it; alessio.faraci@polito.it; gaetano.miraglia@polito.it

* Correspondence: gaetano.miraglia@polito.it

Received: date; Accepted: date; Published: date

Abstract: Bayesian model calibration techniques are commonly employed in the characterization of nonlinear dynamic systems, as they provide a conceptual and effective framework to deal with model uncertainties, experimental errors and procedure assumptions. This understanding has resulted in the need to introduce a model discrepancy term to account for the differences between model-based predictions and real observations. Indeed, the goal of this work is to enhance model-driven Structural Health Monitoring procedures by incorporating the posterior uncertainty linked to updated model discrepancy, and thus make relevant considerations for its use in the Structural Health Monitoring. Specifically, the Bayesian inference has been applied to the calibration of nonlinear hysteretic systems to both provide: (i) most probable values (MPV) of the parameters following the calibration, and; (ii) estimates of the model discrepancy posterior distribution. The effect of the model discrepancy in the calibration is first illustrated recurring to a single degree of freedom Bouc-Wen type oscillator, and then applied for calibrating a reference nonlinear Bouc-Wen model, deriving from real data acquired on a monitored masonry building.

Keywords: Bayesian inference; Uncertainty quantification; Nonlinear hysteretic systems; Bouc-Wen model; Model calibration; Hysteretic system identification; Structural Health Monitoring.

1. Introduction

Models play a key role in simulating the behaviour of engineering structures, though even very detailed models may fail to represent critical mechanisms. The variety of schemes and uncertainties that are typical of civil structures makes the prediction of the actual mechanical behaviour and structural performance a difficult task. All this being said, computer simulations are useful engineering tools to design complex systems and to assess their performance [1]–[3]. These simulations aim at reproducing the underlying physical phenomena in question providing a solution for the governing equations. However, accurate modelling of the structural systems requires them to be calibrated and validated with direct observations and measured experimental data [4].

Most calibration methods are essentially regression techniques that estimate the model parameters based on the outputs, and eventually on the input, by means of various optimization algorithms. Some of the classical approaches of parameter estimation include weighted least-squares estimation, best linear unbiased estimation, etc. [4]. They are nothing but optimization problems of minimizing the difference between computed model output and experimental measured data. However, such deterministic approaches bump into some common problems: they are prone to be

ill-conditioned, extremely susceptible to errors, and affected by stability issues. As a consequence, a single optimal parameter vector is not sufficient to specify the structural model, but rather a family of all plausible values of the model parameters needs to be identified that are consistent with the observations [5]. Moreover, a common situation in practice is to have limited acquired data and hence sparse datasets. This introduces epistemic uncertainty (lack of knowledge) alongside aleatory uncertainty (natural variability) [6]. All these factors result in uncertainty on model prediction. Therefore, addressing the uncertainty in the model parameters, and studying how it influences the uncertainty in the response of the system, is crucial and necessary to get accurate predictions with realistic levels of confidence. This evidence naturally leads to consider the problem from a probabilistic perspective.

The existing literature on probabilistic calibration is extensive [7]–[9] and focuses particularly on Bayesian approaches [10]–[16], Bayesian approaches with model class selection [17] and Bayesian filtering methods [18], [19]. A consequence of using imperfect models in the calibration is that the identified parameters may not correspond to their physical namesakes [1]. The resulting posteriors do not necessarily give estimates of the true value of physical parameters, but rather give values which lead the model to best explain the data. In order to estimate the true physical value of parameters, careful thought needs to be taken when considering which parameters to include in the calibration. In addition, the model discrepancy term must be precisely specified to connect model prediction to the observations [6].

The goal of this work is to enhance model-driven Structural Health Monitoring (SHM) procedures by incorporating the posterior uncertainty linked to updated model discrepancy, in order to propose its use for the SHM of buildings. Specifically, the Bayesian inference has been applied to the calibration of nonlinear hysteretic systems (Section 2). Specifically, the Uncertainty Quantification (UQ) framework developed in [6] is first applied to a numerical benchmark and then on a case study, whose data come from a building monitored within the Italian Seismic Observatory of Structures (OSS) [20] (Section 3). The calibration is conducted exploring different parametric and non-parametric degrading models. Finally, the effect of different levels of degradation on the inference of model parameters is investigated (always in (Section 3) and discussed in Section 4. Conclusions are then drawn in Section 5.

2. Materials and Methods

In the context of Bayesian statistics, it is assumed that all model parameters are random variables. This randomness describes the degree of uncertainty related to their realizations. The inference goal is to draw conclusions making probability statements about the *hypermeters* $\boldsymbol{x}$ given the evidence of actual observations $\boldsymbol{y}$, through *Bayes' theorem*:

$$\pi(\boldsymbol{x} \mid \boldsymbol{y}) = \frac{\pi(\boldsymbol{x})\, \mathcal{L}(\boldsymbol{x}; \boldsymbol{y})}{Z} \tag{1}$$

where $\pi(\boldsymbol{x}|\boldsymbol{y})$ is the posterior distribution of the hyperparameters, $\pi(\boldsymbol{x})$ is their prior distribution and $\mathcal{L}(\mathbf{x}; \mathbf{y})$ is the likelihood function. Z stands for normalizing factor, named evidence or marginal likelihood, that ensures that the distribution $\pi(\boldsymbol{x})$ integrates to 1. Z is defined by the integral $\int_{D_x} \pi(\boldsymbol{x})\, \mathcal{L}(\boldsymbol{x}; \boldsymbol{y})\, dx$. In this way, the solution of the inverse problem coincides with the posterior probability distribution.

2.1. Discrepancy model

In engineering problems, the analysis of physical systems is often performed by means of computational models which are commonly based on analytical equations governing the system or numerical methods. A computational forward model $\mathcal{M}$ is usually defined as a function that maps a set of model input parameters, $\boldsymbol{x}$, governing the system to predict certain output quantities of interest (QoI) $\boldsymbol{y}$. However, forward models are only a mathematical representation of the real system. As a consequence, a discrepancy term shall be introduced to connect model predictions $\mathcal{M}(\boldsymbol{x})$ to the experimental observations $\boldsymbol{y}$ [6], i.e.:

$$\boldsymbol{y} = \mathcal{M}(\boldsymbol{x}) + \varepsilon \tag{2}$$

In this discrepancy term the effects of measurement error on $\boldsymbol{y} \in \boldsymbol{Y}$ and model inaccuracy are gathered. The assumption of additive Gaussian discrepancy with zero mean and residual covariance matrix $\boldsymbol{\Sigma}$ has been made in this work, i.e.:

$$\varepsilon \sim N(\varepsilon \mid 0, \boldsymbol{\Sigma}) \tag{3}$$

$\boldsymbol{\Sigma} = \boldsymbol{\Sigma}(\boldsymbol{x}_\varepsilon)$, where its parameters $\boldsymbol{x}_\varepsilon$ are additional unknowns to infer jointly with the input parameters $\boldsymbol{x}_\mathcal{M}$ of $\mathcal{M}(\boldsymbol{x})$ [6], is a quantity not known a priori, this issue being overcome by parametrizing the residual covariance matrix. A diagonal covariance matrix with unknown residual variances σ^2 is assumed, specifically $\boldsymbol{\Sigma} = \sigma^2 \boldsymbol{I}$. This results in reducing the discrepancy parameter vector in a single scalar, i.e. $\boldsymbol{x}_\varepsilon \equiv \sigma^2$, and in setting the parameter vector as $\boldsymbol{x} = (\boldsymbol{x}_\mathcal{M}, \sigma^2)$. Assuming then a prior distribution $\pi(\sigma^2)$ for the unknown variance of ε, as well as indipendency on the priors of the uncertain model and the discrepancy, the joint prior distribution can be drawn out:

$$\pi(\boldsymbol{x}) = \pi(\boldsymbol{x}_\mathcal{M})\, \pi(\sigma^2) \tag{4}$$

With these assumptions, a particular measurement point $\boldsymbol{y}_\mathrm{i} \in \boldsymbol{Y}$ is a realization of a Gaussian distribution with mean value $\mathcal{M}(\boldsymbol{x})$ and variance σ^2. In this way the likelihood function reads:

$$\mathcal{L}(\boldsymbol{x}_\mathcal{M}, \sigma^2; \boldsymbol{Y}) = N(\boldsymbol{y} \mid \mathcal{M}(\boldsymbol{x}), \sigma^2) \tag{5}$$

Specifically:

$$\mathcal{L}(\boldsymbol{x}_\mathcal{M}, \sigma^2; \boldsymbol{Y}) = \prod_{i=1}^{N} \frac{1}{\sqrt{(2\pi\sigma^2)^N}} e^{-\frac{1}{2\sigma^2}(\boldsymbol{y}_i - \mathcal{M}(\boldsymbol{x}_\mathcal{M}))^T (\boldsymbol{y}_i - \mathcal{M}(\boldsymbol{x}_\mathcal{M}))} \tag{6}$$

where N is the number of measurement points. Hence, the posterior distribution can be computed as:

$$\pi(\boldsymbol{x}_\mathcal{M}, \sigma^2 \mid \boldsymbol{Y}) = \frac{1}{Z} \pi(\boldsymbol{x}_\mathcal{M}) \pi(\sigma^2) \mathcal{L}(\boldsymbol{x}_\mathcal{M}, \sigma^2; \boldsymbol{Y}) \tag{7}$$

which summarizes the updated information about the unknowns as $\boldsymbol{x} = (\boldsymbol{x}_\mathcal{M}, \sigma^2)$ after conditioning on the observation $\boldsymbol{y}$.

2.2. *Bayesian calibration procedure*

In this section, we introduce the key steps of the entire procedure used for the calibration of the stochastic systems examined below (for the numerical benchmark and for the case study). Specifically, a three-phase approach is used as follows:

- Phase 1: definition of the seismic input excitation and of the computational model. Firstly, a ground earthquake acceleration record must be selected as seismic input excitation of the system. Then, one specifies general options for the physical model and its governing laws. In this work the system of Ordinary Differential Equations (ODEs) governing the Bouc-Wen

Peer-reviewed version available at Appl. Sci. 2020, 10, 5813; doi:10.3390/app10175813

hysteretic oscillator (Section 3) are implemented and solved numerically with the explicit Runge-Kutta method.

- Phase 2: definition of the probabilistic prior information on the model parameters. Once defined the computational model $\mathcal{M}(\boldsymbol{x})$, one has to select carefully which model parameters $\boldsymbol{x}_{\mathcal{M}}$ to include in the calibration, in order to get a reliable set of physical values from the resulting posteriors estimates after the Bayesian updating. Prior information on possible values of the hyperparameters are set by setting their prior probability distributions $\pi(\boldsymbol{x}_{\mathcal{M}})$. This is made by defining for each hyperparameter the type of the univariate distribution (i.e. Uniform, Gaussian, Lognormal distributions, etc.) and its statistical moments. The prior information is obtained making some considerations about the amount of the dissipated energy during the hysteresis.
- Phase 3: Bayesian model updating. At this stage, the Bayesian model updating can be carried out using the experimental data $\boldsymbol{Y}$ inferring the posterior distributions of the hyperparameters. However, in many practical applications, a closed form of Equation (7) does not exist. For this reason, Markov Chain Monte Carlo (MCMC) simulations have been conducted herein, allowing to approximate expectation in Equation (8).

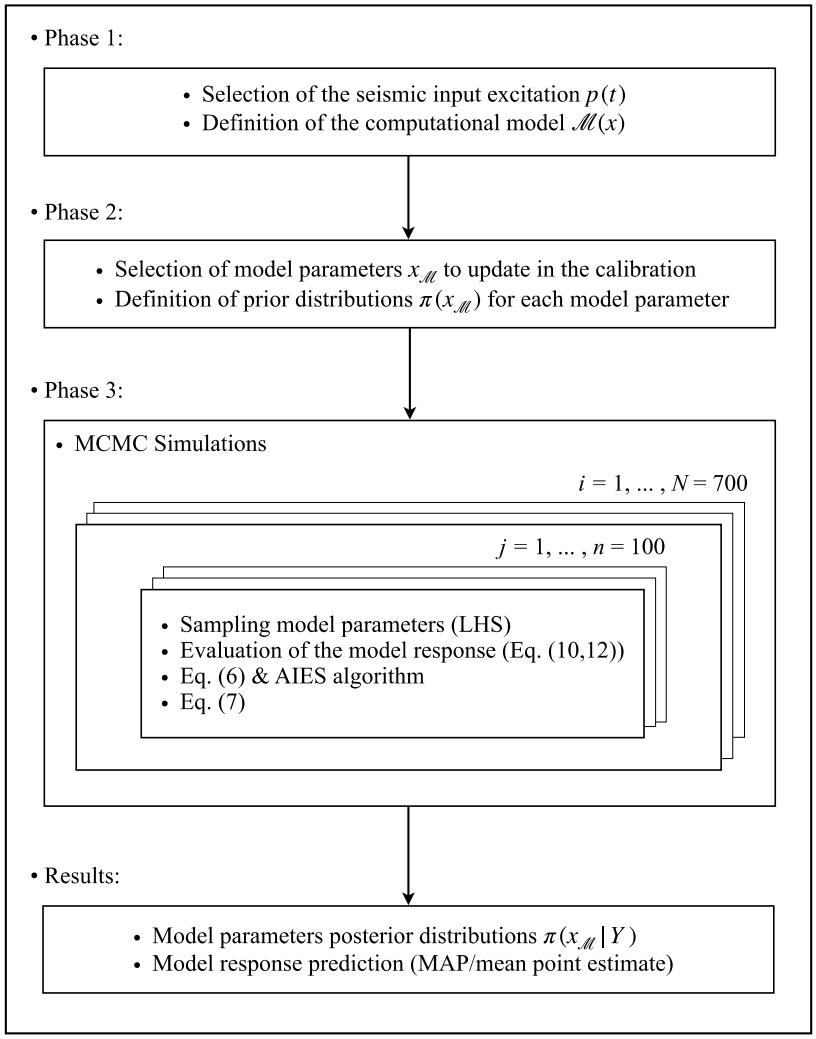

Figure 1. Flowchart of the Bayesian model calibration procedure.

Specifically, the posterior distribution can also be seen as an intermediate quantity used to compute the conditional expectation of a certain Quantity of Interest (QoI) $h(x)$: $D_x \mapsto \mathbb{R}$ [21], so that:

$$\mathbb{E}[h(\boldsymbol{X})|\boldsymbol{Y}] = \int_{D_x} h(\boldsymbol{x})\, \pi(\boldsymbol{x}|\boldsymbol{Y})\, d\boldsymbol{x} \approx \frac{1}{T}\sum_{t=1}^{T} h(\boldsymbol{x}^{(t)}) \tag{8}$$

where $\boldsymbol{x}^{(t)}$ is the step of the chain at iteration t, whereas T is the total number of the generated MCMC samples point. In this way, the posterior is explored by realizing appropriate Markov chains over the prior support. Specifically, the Affine-Invariant Ensemble Sampler (AIES) solver algorithm [22] has been used in this work, and an additive Gaussian discrepancy with zero mean and residual diagonal covariance matrix $\boldsymbol{\Sigma} = \sigma^2 \boldsymbol{I}$ with unknown residual variances σ^2 has been introduced to connect the model response to the experimental observations. To infer σ^2, a uniform prior distribution was assumed:

$$\pi(\sigma^2) \sim U(0, max \mid \boldsymbol{Y} \mid^2) \tag{9}$$

whose standard deviation was set equal to the maximum of the absolute value over the time of the experimental observation $\boldsymbol{Y}$ at the beginning of the calibration. The Bayesian updating is then conducted by minimizing this value, i.e. maximizing the Likelihood function of Equation (6), till the convergence of the Markov chains is reached. The obtained sample can be used to estimate output statistics by drawing samples from the posterior.

Finally, having obtained model parameters posterior distributions, a deterministic model response prediction can be estimated choosing the Maximum a Posteriori (MAP) or the mean of the distributions as point estimate. The aforementioned approach is summarized by the flowchart in Figure 1.

3. Results

3.1. Numerical benchmark: calibration of a SDoF Bouc-Wen type hysteretic system

The Bouc–Wen model of hysteresis is widely used in structural engineering [23]–[28]. The model was proposed by Bouc [29] , and thereafter modified by Wen [30]. The differential equation governing the motion of a Single Degree of Freedom (SDoF) is written in the form:

$$m\ddot{u} + c\dot{u} + f_r(u(t), z(t)) = p(t) \tag{10}$$

where m is the mass of the system, c is the viscous linear damping coefficient, $u(t)$ is the displacement, $f_r(u, z)$ is the restoring force, and $p(t)$ is the external excitation. $\dot{u}(t)$ and $\ddot{u}(t)$ denote derivations in time. According to the Bouc–Wen model, the restoring force is given by the following expression:

$$f_r(u, z) = f_r^{el}(u, z) + f_r^{h}(u, z) = \alpha k_i u(t) + (1 - \alpha) k_i z(t) \tag{11}$$

where $f_r^{el}(u, z)$ represents the elastic component whereas $f_r^{h}(u, z)$ is the hysteretic component, which depends on the past history of the system response, k_i is the initial stiffness of the system, α is the ratio between the final stiffness and initial one, and $z(t)$ is the hysteretic displacement as defined by Baber and Noori in [31] to enhance the capacity of the original model to represent hysteretic cycles:

$$\dot{z}(t) = \frac{A(\varepsilon)\dot{u}(t) - \nu(\varepsilon)[\beta \mid \dot{u}(t) \mid\mid z(t) \mid^{N-1} z(t) + \gamma \dot{u}(t) \mid z(t) \mid^{N}]}{\eta(\varepsilon)} \tag{12}$$

Preprints (www.preprints.org) | NOT PEER-REVIEWED | Posted: 9 July 2020 doi:10.20944/preprints202007.0184.v1

Peer-reviewed version available at Appl. Sci. 2020, 10, 5813; doi:10.3390/app10175813

In Equation (12) the parameters β, γ and N control the shape of the cycles, while the additional parameters $A(\varepsilon)$, $\eta(\varepsilon)$ and $\nu(\varepsilon)$ are degradation functions in terms of the dissipated hysteretic energy $\varepsilon^h(t)$ and take into account the stiffness and strength degradation:

$$A(\varepsilon) = A_0(\varepsilon) - \delta_A \varepsilon^h(t) \tag{13a}$$

$$\nu(\varepsilon) = \nu_0(\varepsilon) - \delta_\nu \varepsilon^h(t) \tag{13b}$$

$$\eta(\varepsilon) = \eta_0(\varepsilon) - \delta_\eta \varepsilon^h(t) \tag{13c}$$

where the constant values of A_0, ν_0, η_0 are usually set to unity [32]. Whereas the values $\delta_A, \delta_\nu, \delta_\eta$ are constant terms which specify the amount of stiffness and strength degradation [33].

Finally, the dissipated hysteretic energy $\varepsilon^h(t)$ is given by:

$$\varepsilon^h(t) = \int_{u(0)}^{u(t)} f_r^h(u,z)du = (1-\alpha)k_i \int_0^t z(\tau)\dot{u}(\tau)d\tau \tag{14}$$

A record of the Montenegro earthquake (1979) was selected from the PEER Ground Motion Database (PEER, 2019) as seismic excitation (Figure 2) for the benchmark.

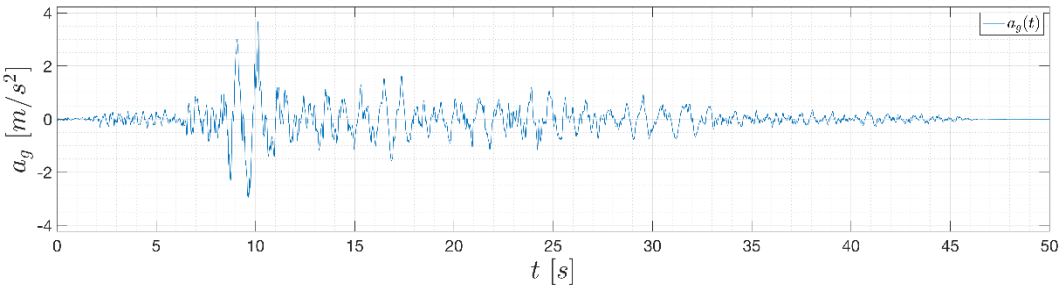

Figure 2. Montenegro (1979) ground motion record with Peak Ground Acceleration (PGA) = 3.59 m/s^2.

This input excitation has been used to simulate the response of a SDoF Bouc-Wen-Baber-Noori (BWBN) nonlinear system with mass of $m = 1200\ kg$. The initial stiffness k_i of the system has been calibrated with the objective of obtaining a plausible system frequency for a masonry structure of approximately $4\ Hz$. A damping ratio of $\xi = 3\ \%$ was adopted. Finally, the remaining BWBN parameters used to generate the simulated record are presented in Table 1, while Figure 3 depicts the simulation record data.

Then the Bayesian calibration has been carried out. Deterministic values are set for the following parameters of the BWBN model: $m = 1200\ kg$, $\xi = 3\ \%$, $A = 1$, $N = 1$. The remaining ones, instead, are considered independent random variables with associated distributions given in Table 2, and constitute the vector of uncertain model parameters $\boldsymbol{x}_M$. It is worth specifying that the degradation effect of the BWBN model has been neglected on purpose, in order to introduce a discrepancy in the model used for emulating the reference response of the system.

The first moments of the prior Probability Density Functions (PDFs) of model parameters k_i and α, namely $\mu_{k_i} = 7.42$ and $\mu_\alpha = 0.063$, have been selected by two linear regressions on the reference restoring force curve for small and high displacements. It is worth noticing that in Table 2 a new random variable γ^* was introduced in order to guarantee the Bounded-Input-Bounded-Output (BIBO) stability [34].

Indeed, assuming as prior knowledge on the parameter γ the required BIBO stability condition, i.e. γ being uniformly distributed between the bounds $-\beta \leq \gamma \leq \beta$, the conditional distribution $\pi(\gamma|\beta)$ must be uniform.

Preprints (www.preprints.org) | NOT PEER-REVIEWED | Posted: 9 July 2020 doi:10.20944/preprints202007.0184.v1

Peer-reviewed version available at Appl. Sci. 2020, 10, 5813; doi:10.3390/app10175813

Table 1. Parameters of the BWBN model adopted for simulating the record data.

$k_i\ (N/m)$	$\beta\ (m^{-1})$	γ	N	δ_A	δ_ν	δ_η
7.6	63	63	1	0	2.43	6.5

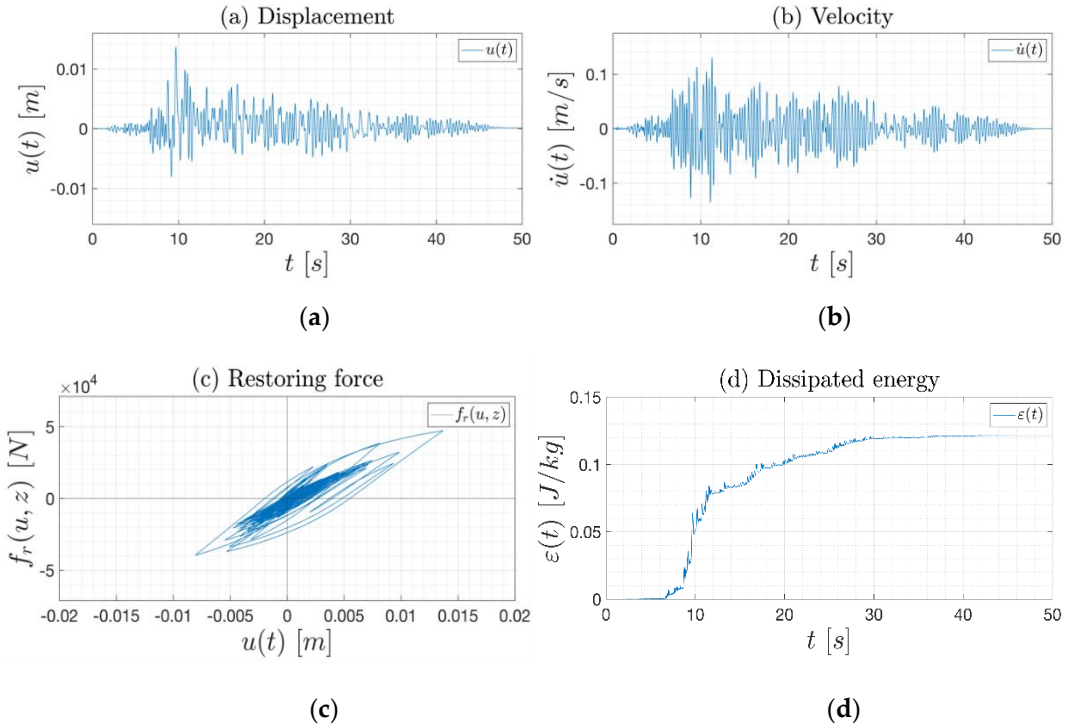

Figure 3. Simulated reference data: (**a**) response displacement of the BWBN oscillator; (**b**) response velocity of the BWBN oscillator; (**c**) hysteresis loop of the BWBN system; (**d**) total dissipated energy of the BWBN system (both elastic and hysteretic components of the restoring force are gathered in) normalized with respect to the mass of the oscillator.

Table 2. Uncertain parameters of the BWBN benchmark model.

Parameter	Distribution	Support	Mean	Std. dev.
$k_i\ (N/m)$	Gaussian	$[4.27, 11.85]$	7.42	0.1
$\beta\ (m^{-1})$	Uniform	$[55, 65]$	60	2.8
γ^*	Uniform	$[-1, 1]$	0	0.57
α	Lognormal	$[0, 1]$	0.063	0.01

$-\beta \leq \gamma \leq \beta$, the conditional distribution $\pi(\gamma|\beta)$ must be uniform. This can be achieved by transforming the input variables, namely removing the parameter γ and introducing an auxiliary variable $\gamma^* \sim U(-1,1)$. Hence, for a joint realization of the parameters β and γ^*, the actual parameter reads: $\gamma = \gamma^*\beta$ for $\beta \neq 0$. To infer the unknown residual variances σ^2 (Equation (9)), a uniform prior distribution was assumed:

$$\pi(\sigma^2) \sim U(0, max \mid \dot{u} \mid^2) \tag{15}$$

whose standard deviation was set equal to the maximum of the absolute value over the time of the experimental observation $\dot{u}$. Markov Chain Monte Carlo (MCMC) simulations have been conducted using MATLAB-based Uncertainty Quantification framework UQLab-V1.3-113® [6] with 100 chains, 700 steps and Affine-Invariant Ensemble Sampler (AIES) solver algorithm [22]. The number of the BWBN forward model $\mathcal{M}^{BW}(\boldsymbol{x})$ calls in MCMC was 70'000. The system of Ordinary

Preprints (www.preprints.org) | NOT PEER-REVIEWED | Posted: 9 July 2020 doi:10.20944/preprints202007.0184.v1

Peer-reviewed version available at Appl. Sci. 2020, 10, 5813; doi:10.3390/app10175813

Differential Equation (ODEs) (Equation (10, 12)) was solved with the MATLAB solver ode45 (explicit Runge-Kutta method with relative error tolerance 1×10^{-3}). Latin hypercube sampling (LHS) method was used to get the parameters prior distributions (Table 2) of the BWBN model, which are shown in Figure 4.

The evolutions of the Markov chains are plotted instead in Figure 5 for each model parameter $\boldsymbol{x} = \{k_i, \beta, \gamma^*, \alpha, \sigma^2\}$; these give valuable insights about convergence of the chains. Indeed, it can be clearly seen as 700 steps are sufficient to reach the steady state. Consequently, samples generated by the chains follow the posterior distributions. However, the sample points generated by the AIES MCMC algorithm have been post-processed carrying out the burn-in of the first half of sample points before convergence to avoid the pollution of the estimate of posterior properties. In our case the quality of the generated MCMC chains can be judged satisfactory. Table 3 reports the result of the Bayesian inversion analysis: mean and standard deviation of the posterior 5%–95% quantiles of the distribution and Maximum A Posteriori (MAP) point estimate. Whereas the posterior distributions of the calibrated parameter are plotted in Fig 6. The MAP can be assumed as the most probable parameter value following calibration. This value has been used as a best-fit parameter.

The model response prediction using MAP as point estimate of the posterior distributions is plotted in Fig 7. It can be clearly seen how the inferred response reproduces the experimental record quite accurately. Actually, we should not dwell upon this specific prediction, rather upon its confidence intervals. The latter tell us how uncertainties on model input propagate through the model.

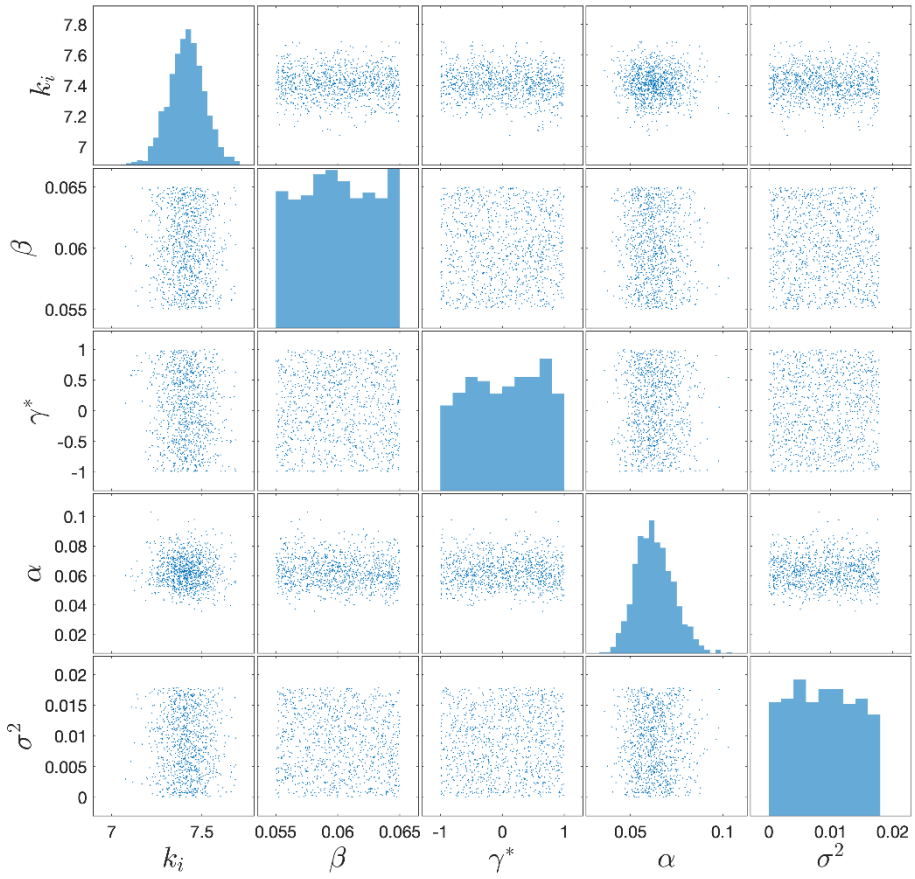

Figure 4. Prior samples of the BWBN benchmark model parameters.

Preprints (www.preprints.org) | NOT PEER-REVIEWED | Posted: 9 July 2020 doi:10.20944/preprints202007.0184.v1

Peer-reviewed version available at Appl. Sci. 2020, 10, 5813; doi:10.3390/app10175813

Table 3. Marginal posterior distribution of the BWBN benchmark model parameters.

Parameter	Mean	Std. dev.	(0.05-0.95) Quant.	MAP
$k_i\ (N/m)$	4.5	0.18×10^{-1}	(4.4 – 4.5)	4.4
$\beta\ (m^{-1})$	65	0.36	$(64 - 65)$	64
γ^*	-0.38	0.25	$(-0.4 - -0.34)$	-0.40
α	0.035	0.53×10^{-2}	(0.027 – 0.044)	0.031
σ^2	2×10^{-4}	4.7×10^{-6}	$(1.9 - 2.1) \times 10^{-4}$	60×10^{-3}

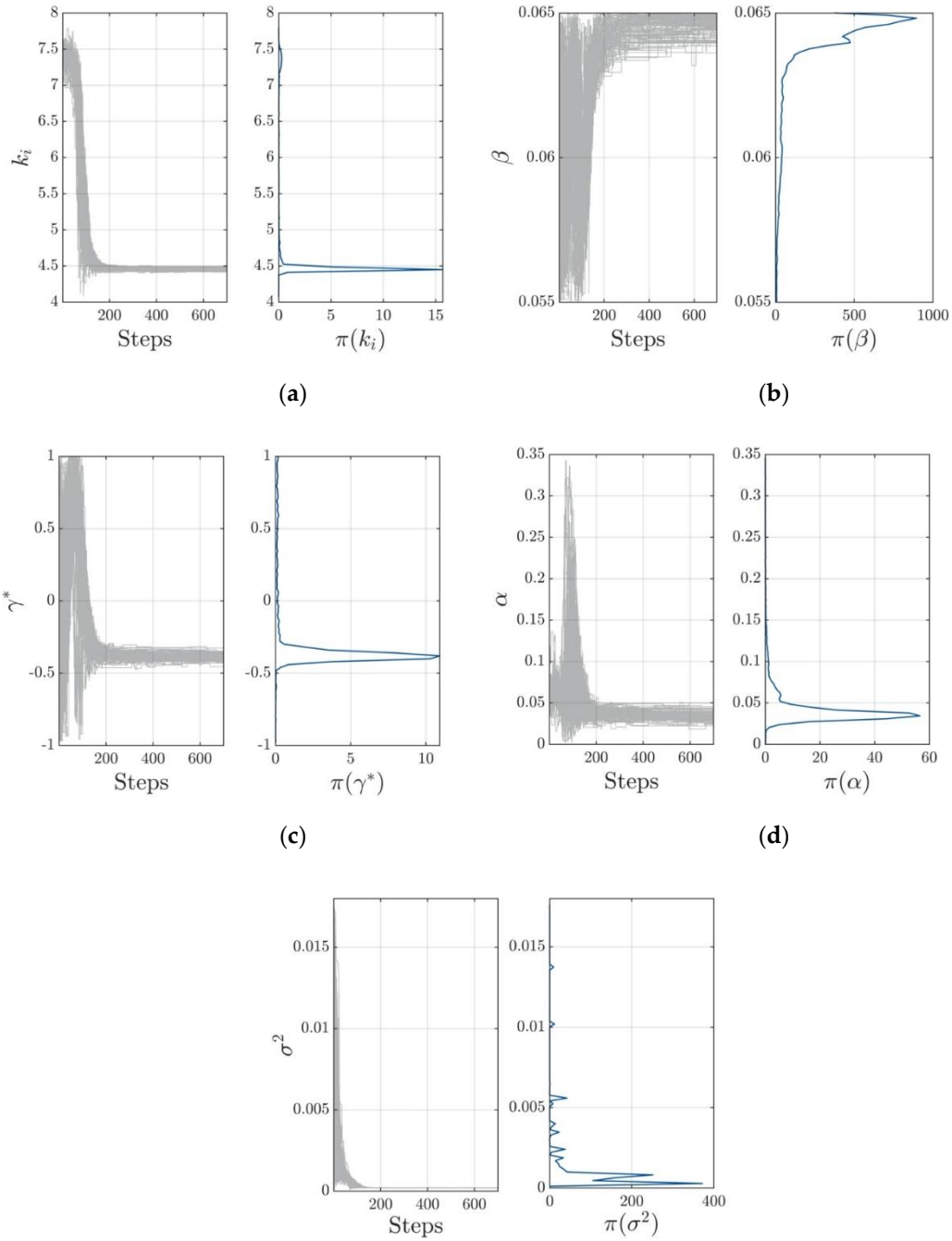

Figure 5. Trace plots of the Markov Chains and corresponding Kernel Density Estimation (KDE) for each BWBN model parameter [6]: (**a**) k_i; (**b**) β; (**c**) γ^*; (**d**) α; (**e**) σ^2.

From the inspection of Figure 7 it can be concluded that uncertainties on the input parameters produce higher uncertainty of the response prediction in the lower amplitude regions rather than in the peak values ones. However, this is a satisfying result in earthquake engineering, where one is more interested in predicting maximum response quantities.

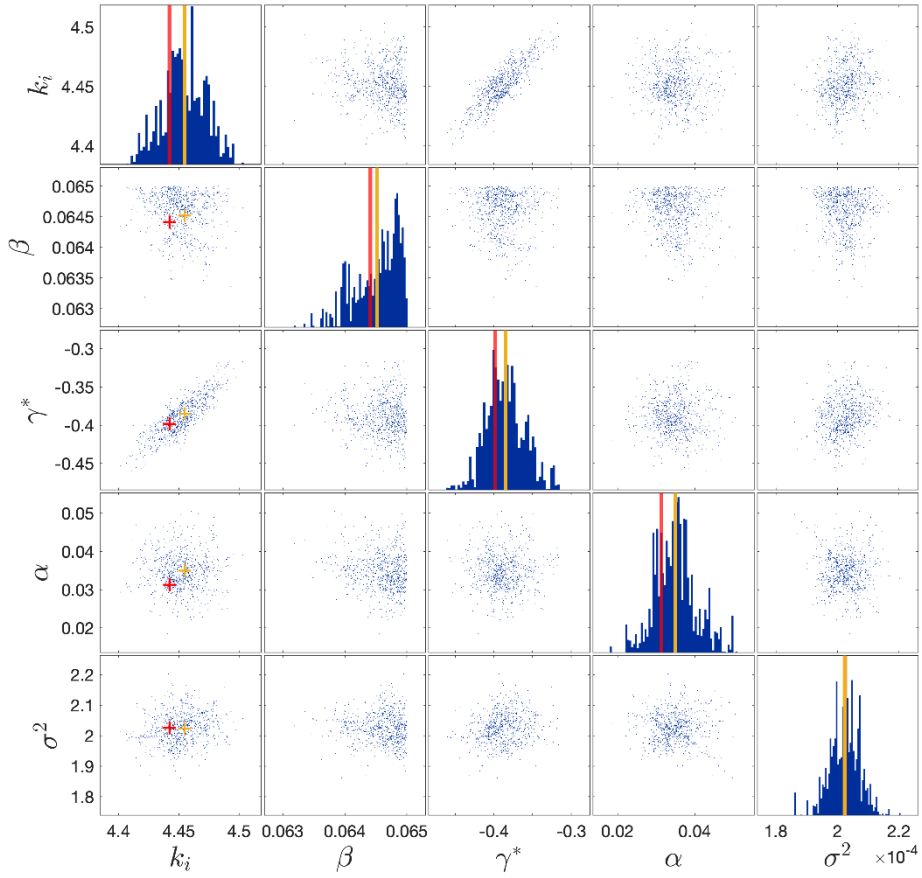

Figure 6. Posterior samples of the BWBN benchmark model parameters: the vertical lines denote the mean of the distribution (in yellow) and the Maximum A Posteriori estimate (MAP) (in red).

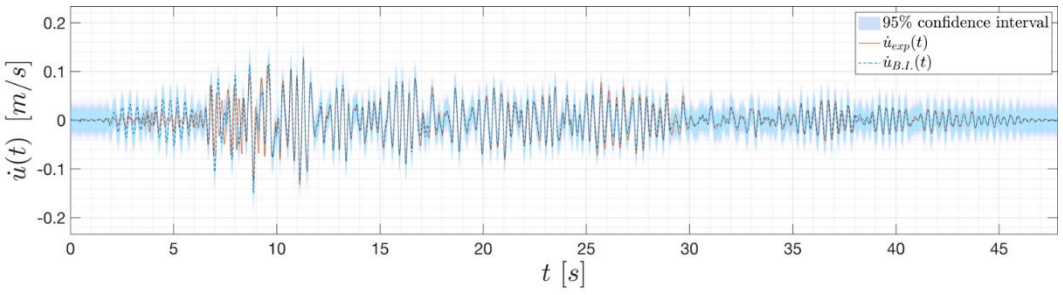

Figure 7. Velocity response prediction of the BWBN benchmark model.

3.2. Demonstration on a case study

Having established that the UQ framework can significantly help to get insight in the uncertainties intrinsic to the calibration, thus furnishing a realistic level of confidence on model prediction, this can now be applied to a case study. The aim is to study the propagation of the discrepancy over an identified hysteretic and degrading model that emulates the experimental response of a real monitored masonry building, the Town Hall of Pizzoli. The latter is a three-story

Preprints (www.preprints.org) | NOT PEER-REVIEWED | Posted: 9 July 2020 doi:10.20944/preprints202007.0184.v1

Peer-reviewed version available at Appl. Sci. 2020, 10, 5813; doi:10.3390/app10175813

stone masonry building located northwest of the city of L'Aquila (Abruzzo), which is away from the city. It was built around 1920 and it formerly hosted a school. The structure presents a u-shaped regular plan, mainly distributed along one direction, and its elevations are characterized by regular openings distributed along three levels above the ground (the raised ground floor, the first floor and the under-roof floor). The total area is about 770 m^2 while the volume is about 5000 m^3. Figure 8 reports the schematizations of the analysed building. The Town Hall of Pizzoli belongs to the network of buildings monitored by OSS [20]. The OSS monitors the structure of Pizzoli thanks to a dynamic monitoring system composed of 8 accelerometers installed on the building and 1 placed at the basement. The acquisition system recorded the sequence that struck central Italy in 2016. For this study, the earthquake acceleration responses of the building recorded on 30-October-2016 are used as reference signals. Since the scope of this study is to show how the discrepancy of models affects the calibration of model parameters value, in what follows only the inter-storey response of the under-roof floor (2nd DoF) has been considered as reference output quantity, being the acceleration of the first floor (1st DoF) the input signal of the reference model. The idea is presenting a numerical case study derived from a real-world structure, with realistic values for hysteretic model parameters.

3.2.1. Reference model

In this subsection the model resulted by a nonlinear identification previously performed on the Pizzoli Town Hall structure is described for completeness. The nonlinear identification, like in [35], [36], relied on a plane frame model in the direction of minor inertia of the building. Assuming the mass contribution of the raised ground floor in the dynamics of the structure is negligible, the building has been modelled with two lumped masses in correspondence of the first and under-roof floor.

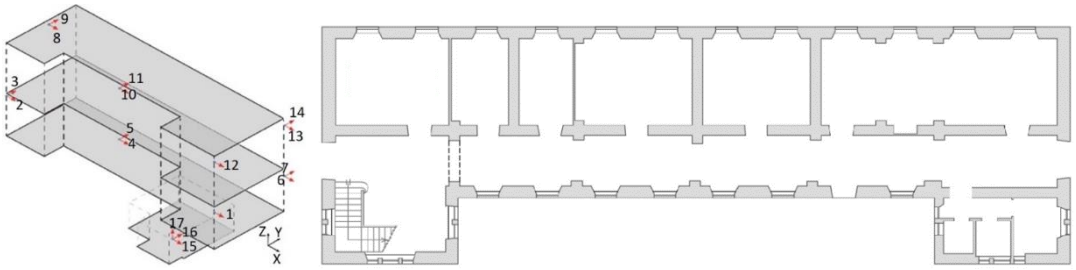

(**a**) (**b**)

Figure 8. Building schematization: (**a**) floors schematization with sensors location; (**b**) plan.

The identification procedure consisted in using absolute acceleration data measured at the floors to approximate the response with a generalized linear model obtained by expanding the Bouc-Wen (BW) model of hysteresis. Actually, the basic functions of the generalized linear model resulted to be nonlinear in terms of the exponential parameters of the BW model. These parameters were therefore identified with specialized optimization algorithms, while for the remaining parameters a direct estimate in the joint time-frequency domain was performed. The identification provided also instantaneous values of the BW model parameters made explicit by the generalized linear model. The main findings of the identification can be summarized as follow:

- The adopted procedure allowed to verify the consistency of the assumed nonlinear model. This was done by checking the stability of the values of the model parameters over the time;

Preprints (www.preprints.org) | NOT PEER-REVIEWED | Posted: 9 July 2020 doi:10.20944/preprints202007.0184.v1

Peer-reviewed version available at Appl. Sci. 2020, 10, 5813; doi:10.3390/app10175813

- The resulting model satisfactorily reproduced the experimental response;
- The procedure allowed to collect timely information on the health of the structure immediately after the occurrence of the earthquake.

In the identification process a global box-like behaviour was assumed, also based on the results of on-site inspections that led to the verification of the existence of good connections between walls and floor-walls, before the occurrence of the seismic events. In addition, no strength deterioration was accounted for (i.e. $\nu(\varepsilon^h) = 1$), while for the stiffness degradation, only the proportional component was maintained, i.e. $\eta(\varepsilon^h) = 1$ and $A(\varepsilon^h) = 1 - \delta_A \varepsilon^h(t)$. The parameter α was instead imposed to zero. Since the aim of this paper is to provide a fuller treatment of the posterior uncertainty linked to the discrepancy applying Bayesian inference to the calibration of nonlinear hysteretic and degrading systems, the reference two DoFs model has been reconducted to a DoF by imposing as input signal the acceleration response of the first floor of the Town Hall (recorded by the monitoring system), $\ddot{u}_1(t)$, and obtaining in output just the inter-story drift, $u(t)$, between the under-roof and the first floor. For further information on the identified model one can refer to [37].

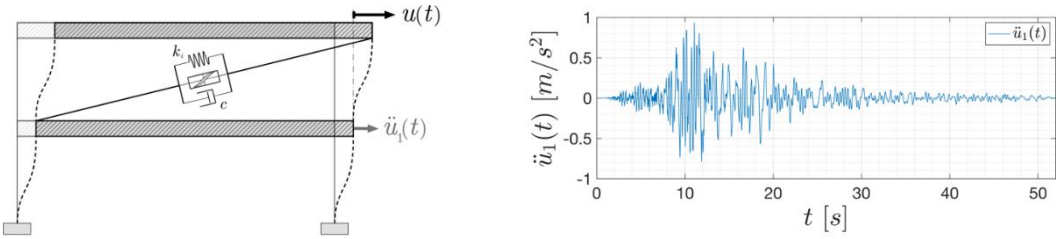

(**a**) (**b**)

Figure 9. Reference model (**a**) structural model; (**b**) acceleration of the first floor.

Thus, the reference model used for the analysis from now on becomes:

$$m \cdot \ddot{u}(t) + f(t) = -m \cdot \ddot{u}_1(t) \tag{16}$$

$$\dot{f}_L(t) = k(\varepsilon^h(t), t) \cdot \dot{u}(t) \tag{17}$$

$$k(\varepsilon^h(t), t) = k_i \cdot (1 - \delta_A \cdot \varepsilon^h(t)) = k_i - k_i \delta_A \cdot \varepsilon^h(t) \tag{18}$$

$$\dot{f}_{NL}(t) = -\beta \dot{u}(t) |f(t)|^N sign[\dot{u}(t) f(t)] - \gamma \dot{u} |f(t)|^N \tag{19}$$

The reference model is depicted in Figure 9 with the acceleration input $\ddot{u}_1(t)$, while the corresponding model parameters, identified in a previous study with the Pizzoli Town Hall building responses, are reported in Table 4. For the numerical simulations, a viscous damping term (with damping ratio of 3%) has been added to the model of Equation (16).

Table 4. Reference model parameters.

Parameter	Value
$k_i\ (N/m)$	5.735e8
$\beta\ (1/m)$	35.01
γ	-16.68
N	1
$\delta_A\ (1/J)$	1.812e-6
$m\ (kg)$	573459

Preprints (www.preprints.org) | NOT PEER-REVIEWED | Posted: 9 July 2020 doi:10.20944/preprints202007.0184.v1

Peer-reviewed version available at Appl. Sci. 2020, 10, 5813; doi:10.3390/app10175813

3.2.2. Bayesian calibration of the reduced single DoF reference model

The reduced single DoF BWBN model has been used to validate the entire procedure in a first phase. Table 5 and 6 report the prior information on model parameters and the results of the Bayesian inversion, respectively.

Table 5. Uncertain parameters of the BWBN model for the case study.

Parameter	Distribution	Support	Mean	Std. dev.
$k_i\ (N/m)$	Lognormal	$[0, \infty]$	6.2×10^2	0.5×10^2
$\beta\ (m^{-1})$	Uniform	$[20, 65]$	4.25	1.3
γ^*	Uniform	$[-1, 1]$	0	0.57
N	Uniform	$[0.1, 2]$	1.05	5.5×10^{-1}
δ_A	Uniform	$[1 \times 10^{-8}, 1 \times 10^{-4}]$	5×10^{-5}	2.88×10^{-5}

Table 6. Marginal posterior distribution of the BWBN model parameters for the case study.

Parameter	Mean	Std. dev.	(0.05-0.95) Quant.	MAP
$k_i\ (N/m)$	5.7×10^2	0.55×10^{-1}	$(5.7 - 5.7) \times 10^2$	5.7×10^2
$\beta\ (m^{-1})$	34	0.26	$(34 - 35)$	34
γ^*	-0.47	0.007	$(-0.49 - -0.46)$	-0.48
N	0.98	0.15	$(0.96 - 1)$	1
δ_A	4.2×10^{-5}	6.8×10^{-6}	$(2.8 - 5.3) \times 10^{-5}$	3.8×10^{-5}
σ^2	1.2×10^{-10}	3.6×10^{-11}	$(0.52 - 1.7) \times 10^{-10}$	3.5×10^{-11}

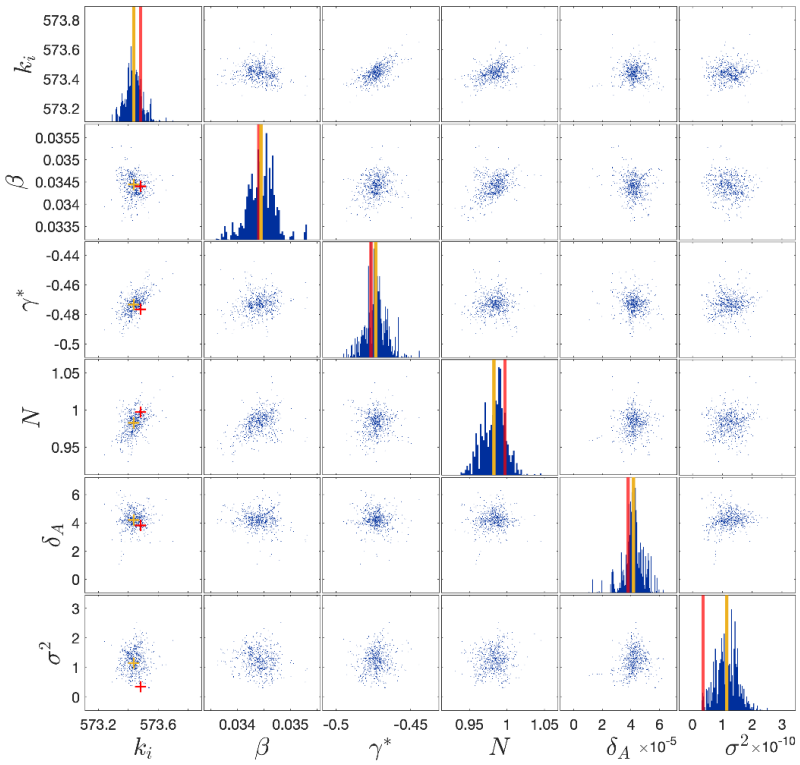

Figure 10. Posterior samples of the BWBN model parameters for the case study: the vertical lines denote the mean of the distribution (in yellow) and the Maximum A Posteriori estimate (MAP) (in red).

Preprints (www.preprints.org) | NOT PEER-REVIEWED | Posted: 9 July 2020 doi:10.20944/preprints202007.0184.v1

Peer-reviewed version available at Appl. Sci. 2020, 10, 5813; doi:10.3390/app10175813

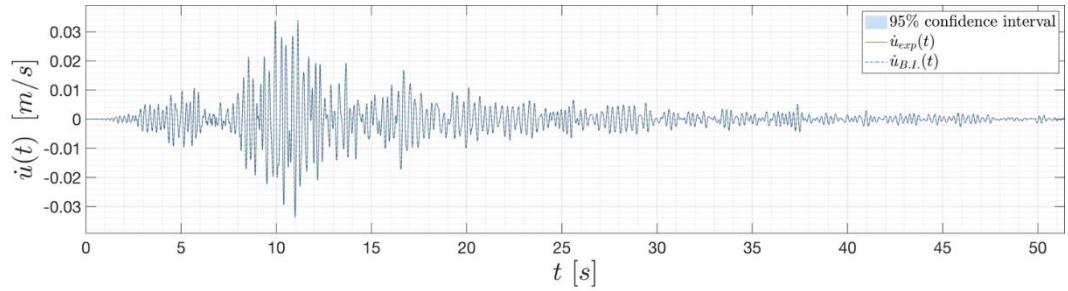

Figure 11. Velocity response prediction of the BWBN model for the case study.

Figure 10 depicts the posterior distributions of the parameters, while Figure 11 depicts the velocity response of the oscillator once the model has been calibrated. From the inspection of the latter, it can be concluded that uncertainties on the input parameters do not affect the response prediction.

Moreover, the value of the degrading term δ_A turns out not to influence the response prediction. This is due to the fact that during the earthquake shaking (PGA $\approx$ 1 m/s²) the structure exhibited a low level of damage [38]. As said before, however, the goal of this work is to investigate how the discrepancy term affects the model response prediction. To this aim, both parametric and non-parametric degradation models have been used herein. Two models per each family are first mathematically introduced, then insights onto the accuracy afforded by each of them are given provided.

3.2.3. Models for stiffness degradation

Besides the original BWBN degrading model, an additional parametric model is now introduced. An important part of the current literature on damage indices focus on exponential function of the dissipated energy.

Consequently, an energy-based exponential function, according to [39], has been used in this work to replace the original BWBN stiffness degradation term $\left(1-\delta_A\varepsilon(t)\right)$ that multiplies the initial stiffness k_i:

$$D_E(t,\varepsilon,\beta)=\exp\left(-\beta\frac{\varepsilon(t)}{\int(-m\ddot{u}-ma_g)dt}\right) \tag{20}$$

where β is an additional parameter to infer jointly with k_i. In order to replicate the degrading effect on the initial stiffness k_i through non-parametric models, probability distribution functions have been used herein. First, according to the procedure used in [40], a Weibull distribution function was adopted:

$$D_W(t,R_W,p_1,p_2)=\left(1-\left[R_W-R_W\,exp\left(-\frac{t}{p_1}\right)_2^{p_2}\right]\right) \tag{21}$$

where R, p_1, p_2 are the distribution parameters to infer jointly with k_i. Meaning to these parameters may be given as follows: p_1 represents the instant of time at which it is experienced the loss of stiffness; p_2 controls its rate; and R_W controls the amount of damage. Secondly, a Logistic distribution function was adopted:

$$D_L(t,R_L,\mu,s)=\left(1-\frac{R_L}{1+exp\left(-\frac{t-\mu}{s}\right)}\right) \tag{22}$$

In this case, parameter μ is the instant of time in which the loss of stiffness occurs, while parameter s represents its rate, and R_L defines the amount of degradation.

Preprints (www.preprints.org) | NOT PEER-REVIEWED | Posted: 9 July 2020 doi:10.20944/preprints202007.0184.v1

Peer-reviewed version available at Appl. Sci. 2020, 10, 5813; doi:10.3390/app10175813

3.2.4. Comparison of the calibrated models

It is useful to make a comparison among all the models introduced to get insights on their accuracy in predicting the response of the oscillator. For the sake of simplicity, from now on, we will refer to: *Model 1*, *Model 2*, *Model 3*, and *Model 4*, to the models with the degrading law of the original BWBN model, of the exponential law, of the Weibull and Logistic distribution functions, respectively. It is worth also to notice that, in order to reduce the number of the parameters to infer, only the initial stiffness k_i and the degrading term have been involved in the calibration process. This can be easily justified by the fact that, for practical earthquake engineering applications, the focus relies on the quantification of the structure's stiffness and its drop (especially for masonry structures which are prone to crack during a seismic event). Prior information on the possible value of the model parameters have been obtained by visual inspection of the dissipated energy vs time curve. For both parametric and non-parametric models, the velocity response of the system obtained is almost identical to the one of Figure 11 for a low-level of degradation. Figure 12 depicts the posterior distributions of the initial stiffness parameter k_i for each model considered. From this inspection, it can be noticed how all the models are able to predict the correct value of the initial stiffness. The choice of the MAP (or of the mean of the distributions) as point estimate after the uncertainty propagation leads to underrate slightly the initial stiffness regardless the model adopted. However, this is neglectable from an engineering point of view. Moreover, Figure 12 depicts the distributions of the discrepancy variance term σ^2 as well. It can be noticed as all the models share the same order of magnitude for σ^2 and, more or less, the same variance. This can be read as follows: the adopted Gaussian discrepancy term, with mean null and unknown variance, performs as a good function to embody all the model errors arising. Thus, at the end, it appears clear how the choice of the model used to infer the stiffness of the oscillator is not meaningful in the presence of a low-level of damage.

3.3. Influence of the degradation level on model parameters inference

Having established that the choice of the models used to infer the stiffness parameter k_i appears to be not relevant for a low-level of degradation, the aim is now to investigate what happens in possible further scenarios in which higher level of damage is exhibited. To this aim, the input excitation has been rescaled. Specifically, two cases are examined as follows: (i) one in which the input has been rescaled with a PGA of 6 m/s² (medium level of degradation); (ii) and one in which the input has been rescaled with a PGA of 9 m/s² (high level of degradation).

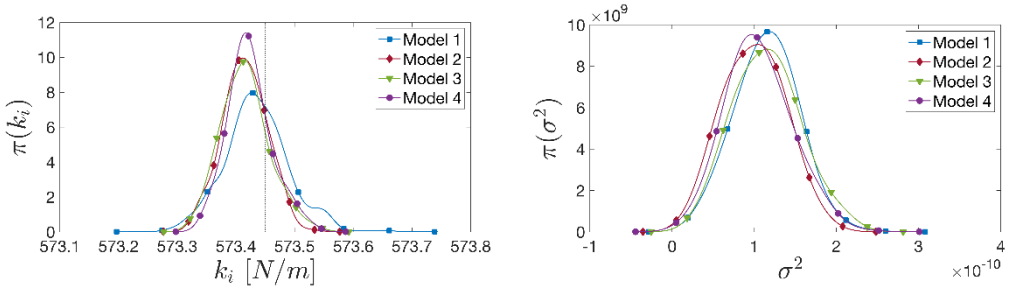

(**a**) (**b**)

Preprints (www.preprints.org) | NOT PEER-REVIEWED | Posted: 9 July 2020 doi:10.20944/preprints202007.0184.v1

Peer-reviewed version available at Appl. Sci. 2020, 10, 5813; doi:10.3390/app10175813

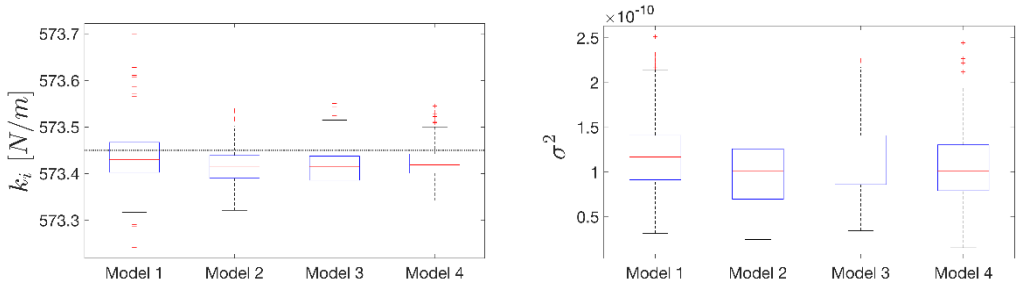

(**c**) (**d**)

Figure 12. (**a**) Kernel Density Estimations (KDE) of the initial stiffness model parameter k_i (on the left) and; (**b**) of the discrepancy variance σ^2 for each model (low-level of degradation, PGA $\approx$ 1 m/s2). (**c**) boxplot representations (based on the five-number summary: minimum, first quartile, median, third quartile, and maximum) of the posterior samples for the model parameter k_i and; (**d**) σ^2. The horizontal and vertical dotted lines in the plots represent the calibrated reference value of k_i.

3.3.1. Medium level of degradation

Increasing the level of the excitation to a medium value (i.e. PGA of 6 m/s²) and keeping the same reference damage, all the models are still able to predict the correct value of the initial stiffness k_i. However, an increase of the uncertainties in the model prediction is registered, this time due to the greater values of the discrepancy variance. The choice of the MAP (or of the mean of the distributions) as point estimate now leads to overrate slightly the initial stiffness. Being the estimation error negligible, the adopted discrepancy term still performs as a good function to embody all the model errors. However, increasing the level of the input without accounting for a growth of the damage level appears to be unrealistic. This because higher seismic excitations generally involve greater dissipation of energy. Therefore, a loss up to the 40% of the initial stiffness k_i has been taken into account as well, this resulting in Model 1, i.e. the one consistent with the BWBN degrading model, being able to predict the correct value of the initial stiffness; on the contrary, all the models that are inconsistent with the BWBN one (i.e. Model 2, 3, and 4) overrate the initial stiffness value in a no longer negligible proportion (Figure 13), leading to higher level of uncertainty in the model response prediction. It is also worth noticing how the estimation error is amplified for non-parametric models. This is a considerable indicator of the inadequacy of the discrepancy function adopted. In order to recover the response records, more accurate and well-suited discrepancy models should be investigated, but this is out of the purpose of this work.

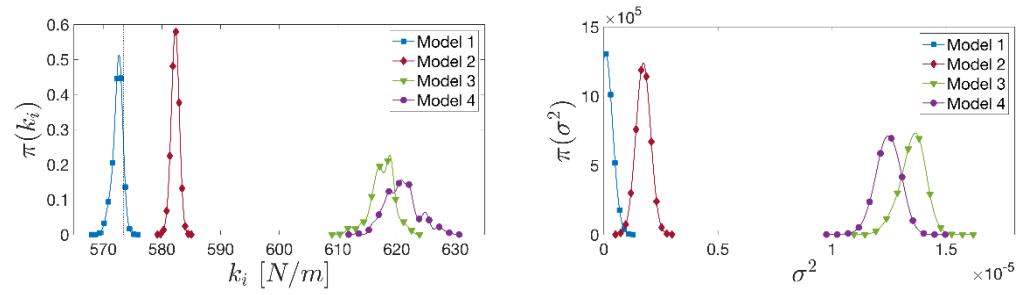

(**a**) (**b**)

Preprints (www.preprints.org) | NOT PEER-REVIEWED | Posted: 9 July 2020 doi:10.20944/preprints202007.0184.v1

Peer-reviewed version available at Appl. Sci. 2020, 10, 5813; doi:10.3390/app10175813

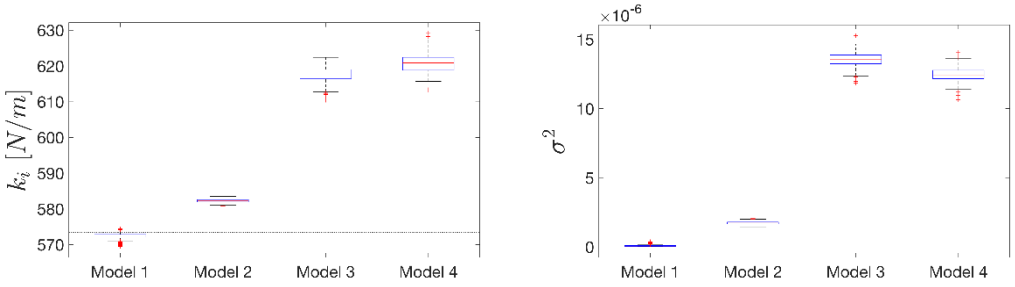

(**c**) (**d**)

Figure 13. (**a**) Kernel Density Estimations (KDE) of the initial stiffness model parameter k_i and; (**b**) of the discrepancy variance σ^2 for each model (medium-level of degradation: PGA $\approx$ 6 m/s2, stiffness reduction up to 40% of the initial one). (**c**) boxplot representations (minimum, first quartile, median, third quartile, and maximum) of the posterior samples for the model parameter k_i and; (**d**) σ^2. The horizontal and vertical dotted lines in the plots represent the calibrated reference value of the initial stiffness.

3.3.2. High level of degradation

A further and final step consisted in increasing the level of the input to a high value, i.e. PGA of 9 m/s^2. Again, when keeping the same level of the reference damage, all models are able to predict the correct value of the initial stiffness although with a visible greater variance than before. When the level of damage is increased taking into account a stiffness loss up to the 80% of the initial one, the same conclusions made in Section 3.3.1 are confirmed also in this case, stressing the fact that now the level of uncertainty is greater due to both greater excitation and a higher level of damage.

4. Discussion

Resuming, it has been determined from the analysis on a realistic case study that a Gaussian discrepancy term, with null mean and unknown variance, is an effective choice in order to tackle the model inaccuracy rising for low levels of degradation when the aim is the inference of the system's initial stiffness. At the same time, it has been proven that this kind of discrepancy still works fine for low levels of damage even if the input is rescaled up to $1g$. Consequently, the discrepancy term adopted can be judged suitable to cover model errors with increasing values of the PGA. Of course, however, higher levels of PGA introduce higher uncertainties in the model prediction. Moreover, it has been shown that an increase in the amount of degradation jointly to the increase of the damage lead to inaccurate predictions for those models that are inconsistent with the original physical BWBN model, and much more uncertainties in the latter. This can be appreciated, for example, in the velocity response prediction of Model 3 (Figure 14). Precisely, this model is the one leading to the worst model prediction for high level of degradation, owing to the presence of a greater number of overestimated outliers. At last, for those cases it can be concluded that the simple discrepancy function adopted is not sufficient to embody all the model errors and, therefore, a specific model for the mean of the discrepancy term should be introduced to cover them. This means that the choice of the discrepancy function should be linked to the level of damage and, in actual practice applications, to the level of excitation. This finding could stimulate further researches on the statistical correlation of discrepancy models and magnitude of excitation, helping in this way the calibration of mathematical models that try to emulate real word systems and structures.

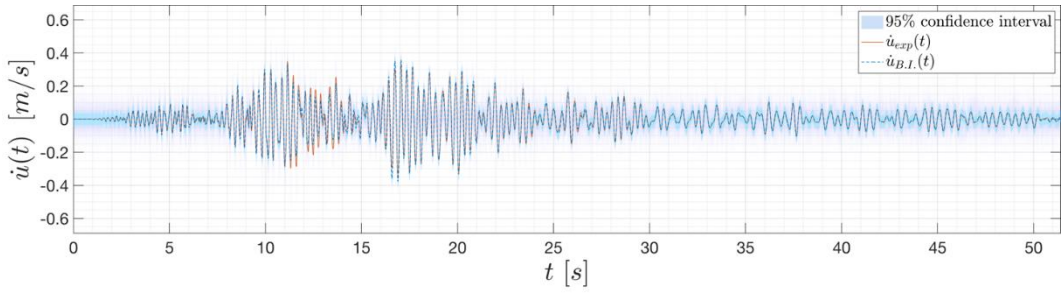

Figure 14. Velocity response prediction of the BWBN Model 3 for high level of degradation (PGA of 9 m/s², stiffness reduction up to 80% of the initial one).

5. Conclusions

This article addressed the Bayesian probabilistic calibration of nonlinear hysteretic systems for model-driven SHM purposes. The model calibration procedure is enhanced by incorporating the posterior uncertainty linked to model discrepancy. The effect of the model discrepancy in the calibration was first illustrated with a single degree of freedom Bouc-Wen type oscillator, and then applied to a reference model derived from a calibrated 2 degrees of freedom system of a real monitored masonry building hit by the 2016 Central Italy earthquake. The Bayesian inference performed on the examined cases, provided the most probable values of the parameters following the calibration, as well as an estimate of the model discrepancy posterior distribution. Furthermore, with reference to the case study associated to Pizzoli Town Hall, several parametric and non-parametric degrading models were investigated to get insights on how model inaccuracy could be embodied by the discrepancy function adopted. It has been determined that a Gaussian discrepancy term, with null mean and unknown variance, is unable to tackle the model inaccuracy rising for high levels of damage. Consequently, for these cases, the use of a fuller and specific model for the mean of the discrepancy term to get reliable estimates should be used. On the contrary, for low level of damage, and even for high levels of PGA, it has been demonstrated that accurate predictions can be achieved thanks to this discrepancy model, which overcomes the low sensitivity of the term used to model the degradation in the response. Moreover, when the magnitude of the external excitation is very high (for the system considered), or the system is subjected to resonance, the system is likely to undergo damage (e.g. to high level of degradation) and thus simplified assumptions on the model discrepancy term are not reasonable.

These results suggest further studies to better relate discrepancy models to the statistical nature of the excitation and other factors that can influence probabilistic model calibration for use in structural health monitoring.

Author Contributions: Methodology, Alessio Faraci; Case study, Alessio Faraci and Gaetano Miraglia; Review, Rosario Ceravolo and Gaetano Miraglia, Editing, Alessio Faraci; Supervision, Rosario Ceravolo. All authors have read and agreed to the published version of the manuscript.

Funding: This research received no external funding.

Acknowledgments: The data of the Town Hall of Pizzoli were supplied by the Seismic Observatory of Structures within the DPC-ReLUIS project. Computational resources were provided by HPC@POLITO (http://hpc.polito.it).

Conflicts of Interest: The authors declare no conflict of interest.

References

[1] L. Biegler *et al.*, "Large-scale inverse problems and quantification of uncertainty," vol. 712. Wiley Online

Library, 2011.

[2] G. Bernagozzi, S. Mukhopadhyay, R. Betti, L. Landi, and P. P. Diotallevi, "Output-only damage detection in buildings using proportional modal flexibility-based deflections in unknown mass scenarios," *Eng. Struct.*, 2018, doi: 10.1016/j.engstruct.2018.04.036.

[3] Y. Liu *et al.*, "Seismic behaviour and failure-mode-prediction method of a reinforced-concrete rigid-frame bridge with thin-walled tall piers: Investigation by model-updating hybrid test," *Eng. Struct.*, 2020, doi: 10.1016/j.engstruct.2020.110302.

[4] N. Catbas, T. Kijewski-Correa, and A. Aktan, "Structural Identification of Constructed Systems - Approaches, Methods, and Technologies for Effective Practice of St-Id." American Society of Civil Engineers (ASCE), 2013, doi: 10.1061/9780784411971.

[5] J. L. Beck and L. S. Katafygiotis, "Updating models and their uncertainties. I: Bayesian statistical framework," *J. Eng. Mech.*, 1998, doi: 10.1061/(ASCE)0733-9399(1998)124:4(455).

[6] P.-R. Wagner, J. Nagel, S. Marelli, and B. Sudret, "UQLab user manual - Bayesian inversion for model calibration and validation." Chair of Risk, Safety and Uncertainty Quantification, ETH Zurich, Switzerland, 2019.

[7] J.-P. Noël and G. Kerschen, "Nonlinear system identification in structural dynamics: 10 more years of progress," *Mech. Syst. Signal Process.*, vol. 83, pp. 2–35, 2017.

[8] J. Ching, J. L. Beck, and K. A. Porter, "Bayesian state and parameter estimation of uncertain dynamical systems," *Probabilistic Eng. Mech.*, vol. 21, no. 1, pp. 81–96, 2006.

[9] G. A. Ortiz, D. A. Alvarez, and D. Bedoya-Ru\'\iz, "Identification of Bouc--Wen type models using the transitional Markov chain Monte Carlo method," *Comput. Struct.*, vol. 146, pp. 252–269, 2015.

[10] H. P. Chen and M. B. Mehrabani, "Reliability analysis and optimum maintenance of coastal flood defences using probabilistic deterioration modelling," *Reliab. Eng. Syst. Saf.*, 2019, doi: 10.1016/j.ress.2018.12.021.

[11] K. Erazo and S. Nagarajaiah, "An offline approach for output-only Bayesian identification of stochastic nonlinear systems using unscented Kalman filtering," *J. Sound Vib.*, 2017, doi: 10.1016/j.jsv.2017.03.001.

[12] K. Zhou and J. Tang, "Uncertainty quantification in structural dynamic analysis using two-level Gaussian processes and Bayesian inference," *J. Sound Vib.*, 2018, doi: 10.1016/j.jsv.2017.09.034.

[13] G. Yan and H. Sun, "A non-negative Bayesian learning method for impact force reconstruction," *J. Sound Vib.*, 2019, doi: 10.1016/j.jsv.2019.06.013.

[14] W. J. Yan, D. Chronopoulos, C. Papadimitriou, S. Cantero-Chinchilla, and G. S. Zhu, "Bayesian inference for damage identification based on analytical probabilistic model of scattering coefficient estimators and ultrafast wave scattering simulation scheme," *J. Sound Vib.*, 2020, doi: 10.1016/j.jsv.2019.115083.

[15] M. Imholz, M. Faes, D. Vandepitte, and D. Moens, "Robust uncertainty quantification in structural dynamics under scarse experimental modal data: A Bayesian-interval approach," *J. Sound Vib.*, 2020, doi: 10.1016/j.jsv.2019.114983.

[16] Ç. Hızal and G. Turan, "A two-stage Bayesian algorithm for finite element model updating by using ambient response data from multiple measurement setups," *J. Sound Vib.*, 2020, doi: 10.1016/j.jsv.2019.115139.

[17] M. Muto and J. L. Beck, "Bayesian updating and model class selection for hysteretic structural models using stochastic simulation," *J. Vib. Control*, vol. 14, no. 1–2, pp. 7–34, 2008.

[18] M. Wu and A. W. Smyth, "Application of the unscented Kalman filter for real-time nonlinear structural system identification," *Struct. Control Heal. Monit. Off. J. Int. Assoc. Struct. Control Monit. Eur. Assoc.*

Control Struct., vol. 14, no. 7, pp. 971–990, 2007.

[19] R. Astroza, H. Ebrahimian, and J. P. Conte, "Material parameter identification in distributed plasticity FE models of frame-type structures using nonlinear stochastic filtering," *J. Eng. Mech.*, vol. 141, no. 5, p. 4014149, 2015.

[20] M. Dolce, M. Nicoletti, A. De Sortis, S. Marchesini, D. Spina, and F. Talanas, "Osservatorio sismico delle strutture: the Italian structural seismic monitoring network," *Bull. Earthq. Eng.*, 2017, doi: 10.1007/s10518-015-9738-x.

[21] S. Marelli and B. Sudret, "UQLab: A Framework for Uncertainty Quantification in Matlab." 2014, doi: 10.1061/9780784413609.257.

[22] J. Goodman and J. Weare, "Communications in Applied Mathematics and Computational Science," *Math. Sci. Publ.*, 2010.

[23] A. Kyprianou, K. Worden, and M. Panet, "Identification of hysteretic systems using the differential evolution algorithm," *J. Sound Vib.*, 2001, doi: 10.1006/jsvi.2001.3798.

[24] K. Worden and J. J. Hensman, "Parameter estimation and model selection for a class of hysteretic systems using Bayesian inference," *Mech. Syst. Signal Process.*, 2012, doi: 10.1016/j.ymssp.2012.03.019.

[25] A. Ben Abdessalem, N. Dervilis, D. Wagg, and K. Worden, "Model selection and parameter estimation in structural dynamics using approximate Bayesian computation," *Mech. Syst. Signal Process.*, 2018, doi: 10.1016/j.ymssp.2017.06.017.

[26] R. Ceravolo, G. V. Demarie, and S. Erlicher, "Instantaneous identification of degrading hysteretic oscillators under earthquake excitation," *Struct. Heal. Monit.*, 2010, doi: 10.1177/1475921710368202.

[27] R. Ceravolo, G. V. Demarie, and S. Erlicher, "Instantaneous identification of Bouc-Wen-type hysteretic systems from seismic response data," in *Key Engineering Materials*, 2007, doi: 10.4028/0-87849-444-8.331.

[28] R. Ceravolo, G. V. Demarie, and S. Erlicher, "Identification of degrading hysteretic systems from seismic response data," in *7th European Conference on Structural Dynamics, EURODYN 2008*, 2008.

[29] R. Bouc, "Modèle mathématique d'hystérésis: application aux systèmes à un degré de liberté," *Journal Acustica*, vol. 24. pp. 16–25, 1969.

[30] Y.-K. Wen, "Method for Random Vibration of Hysteretic Systems," *Journal of Engineering Mechanics Division ASCE*, vol. 102, no. 2. pp. 249–263, 1976.

[31] T. T. Baber and M. N. Noori, "Random Vibration of Degrading, Pinching Systems," *Journal of Engineering Mechanics*, vol. 111, no. 8. pp. 1010–1026, 1985.

[32] F. Ma, H. Zhang, A. Bockstedte, G. C. Foliente, and P. Paevere, "Parameter analysis of the differential model of hysteresis," *J. Appl. Mech. Trans. ASME*, 2004, doi: 10.1115/1.1668082.

[33] S. Erlicher and O. S. Bursi, "Bouc-Wen-type models with stiffness degradation: Thermodynamic analysis and applications," *J. Eng. Mech.*, 2008, doi: 10.1061/(ASCE)0733-9399(2008)134:10(843).

[34] F. Ikhouane and J. Rodellar, "Systems with Hysteresis: Analysis, Identification and Control Using the Bouc-Wen Model." 2007, doi: 10.1002/9780470513200.

[35] O. S. Bursi, R. Ceravolo, S. Erlicher, and L. Zanotti Fragonara, "Identification of the hysteretic behaviour of a partial-strength steel--concrete moment-resisting frame structure subject to pseudodynamic tests," *Earthq. Eng. Struct. Dyn.*, vol. 41, no. 14, pp. 1883–1903, 2012.

[36] R. Ceravolo, S. Erlicher, and L. Z. Fragonara, "Comparison of restoring force models for the identification of structures with hysteresis and degradation," *J. Sound Vib.*, vol. 332, no. 26, pp. 6982–6999, 2013.

[37] G. Miraglia, E. Lenticchia, S. Cecilia, and R. Ceravolo, "Seismic Damage Identification by Fitting the

Nonlinear and Hysteretic Dynamic Response of Monitored Buildings," *J. Civ. Struct. Heal. Monit.*, vol. 0, no. 0, p. 0, 2020.

[38] S. Cattari *et al.*, "Discussion on data recorded by the Italian structural seismic monitoring network on three masonry structures hit by the 2016-2017 central Italy earthquake," in *COMPDYN Proceedings*, 2019, vol. 1, pp. 1889–1906.

[39] A. Colombo and P. Negro, "A damage index of generalised applicability," *Eng. Struct.*, 2005, doi: 10.1016/j.engstruct.2005.02.014.

[40] J. Deng and D. Gu, "On a statistical damage constitutive model for rock materials," *Comput. Geosci.*, 2011, doi: 10.1016/j.cageo.2010.05.018.